Isotopic Exchange in CH_4–D_2 and CD_4–H_2 Mixtures Studied by Ion Cyclotron Resonance Spectroscopy. The Mechanism of Self-Induced Labeling of Methane by Tritium[1]

M. Inoue and S. Wexler

Contribution from the Department of Chemistry, Argonne National Laboratory, Argonne, Illinois 60439. *Received March 26, 1969*

Abstract: The mechanisms of isotopic exchange of hydrogen atoms in the ionic reactions in CH_4–D_2 and in CD_4–H_2 mixtures have been investigated by the technique of ion cyclotron resonance spectroscopy. The chains of competitive and consecutive ion–molecule reactions leading from the primary ions produced by electron impact to ethyl ions with none, one, two, or three of their hydrogen atoms replaced by deuterium were established from studies of CH_4–D_2 mixtures and confirmed with CD_4–H_2 mixtures. Isotopically labeled methyl ions are formed in reactions of D_3^+ with CH_4 and of methyl ions with D_2, and these then react with methane to give the labeled ethyl ions. The latter are inert toward D_2 and only slightly reactive with CH_4. Xenon and nitric oxide inhibit the production of the tagged ethyl ions initiated by reactions of D_2^+ and D_3^+, but have little effect on their formation by chains of reactions beginning with CH_3^+ from methane. The sequences of ionic reactions observed should be the same as those which occur in the "Wilzbach labeling" of methane by tritium, in which tritium is present rather than deuterium, and the ionization and excitation are initiated internally by β particles and secondary electrons. Mechanisms involving only ionic and ionic followed by free-radical reactions are proposed for the Wilzbach labeling of methane.

More than 10 years ago Wilzbach[2] demonstrated a simple and widely applicable method for labeling organic molecules with radioactive tritium. Mixtures of the compound and T_2 were prepared and allowed to stand, and the various tritiated products were then separated and identified by radio gas chromatography.[2,3] Because of the great interest in these fundamental hydrogen-exchange reactions, as well as the widespread practical application of the method for tagging complex molecules of biological and medical importance,[4] several studies of the mechanisms of "Wilzbach labeling" have been reported. Gant and Yang[5] have investigated the kinetics of tritiation of several of the lower hydrocarbons by conventional techniques, and methane in particular has been studied by Pratt and Wolfgang.[6] The conclusion of both pairs of workers was that two modes of tagging were involved: decay-induced labeling initiated by the reactivity of the $(T\,He^3)^+$ daughter formed directly from the nuclear transformation of T_2; and radiation-induced labeling, which is caused by excitation and ionization of the compound and T_2 by β particles released in the nuclear decays and by secondary electrons, *i.e.*, self-induced radiolysis of the mixture. Both mechanisms were invoked to account for production of the tagged substrate molecule as well as the formation of other products observed. Methane–tritium gaseous mixtures have also been investigated by Cacace, *et al.*,[7] under conditions where the decay-induced mechanism was dominant. Positively charged transient species were assumed to be involved as intermediates in the proposed mechanisms. A somewhat related investigation of exchange of deuterium atoms with the methane in mixtures of $CH_4 + D_2$ irradiated as a result of β decay of added tritium was conducted by Firestone, Lemr, and Trudel,[8] who proposed an ion–molecule chain mechanism to account for the formation of CH_3D below 123°.

If the ions suggested as intermediates in the isotopic exchange are long-enough lived to survive for the time required for them to travel from the source chamber of a magnetic sector mass spectrometer to its detector, a time of about 10^{-5} sec, they should be observable and subject to study by the techniques of "high-pressure" mass spectrometry, in which the pressure in the source is sufficiently great that consecutive ion–molecule reactions can occur. Several investigations of this nature have been published in recent years,[9–11] in which mass spectra have been recorded as a function of composition of gas mixture and of energy of ionizing electrons. Although many of the ionic intermediates, mainly isotopically labeled methyl and ethyl ions, formed in the exchange of hydrogen atoms in methane have been identified, and the rate constants for some of their reactions measured, the complexity of the modes of concurrent consecutive and competitive ion–molecule reactions often left ambiguous the exact mechanisms involved.

It appeared to the authors that the new technique of ion cyclotron resonance spectroscopy (icr)[12–14] would help overcome the difficulties inherent in the former approach, and a clearer understanding of the mechanisms of isotopic exchange occurring in Wilzbach labeling might come from restudy of these gaseous systems by

(1) Work performed under the auspices of the U. S. Atomic Energy Commission.
(2) K. E. Wilzbach, *J. Am. Chem. Soc.*, **79**, 1013 (1957); K. E. Wilzbach and P. Riesz, *J. Phys. Chem.*, **62**, 6 (1958).
(3) W. R. Ahrens, M. C. Sauer, and J. E. Willard, *J. Am. Chem. Soc.*, **79**, 3284 (1957).
(4) See, for example, "Proceedings of the 5th Annual Symposium on Advances in Tracer Technology," Vol. I, R. Rothchild, Ed., Plenum Press, New York, N. Y., 1963.
(5) P. L. Gant and K. Yang, *J. Chem. Phys.*, **32**, 1757 (1960); **31**, 1589 (1959); **30**, 1108 (1959); *J. Phys. Chem.*, **66**, 1619 (1962).
(6) T. H. Pratt and R. Wolfgang, *J. Am. Chem. Soc.*, **83**, 10 (1961).
(7) F. Cacace, R. Cipollini, and G. Ciranni, *ibid.*, **90**, 1122 (1968).
(8) R. F. Firestone, C. F. Lemr, and G. J. Trudel, *ibid.*, **84**, 2279 (1962).
(9) S. Wexler, *ibid.*, **85**, 272 (1963); "Proceedings of the Symposium on Exchange Reactions," International Atomic Energy Agency, Vienna, 1965, p 301.
(10) M. S. B. Munson, F. H. Field, and J. L. Franklin, *J. Am. Chem. Soc.*, **85**, 3584 (1963).
(11) V. Aquilanti and G. G. Volpi, *J. Chem. Phys.*, **44**, 2307 (1966).
(12) L. R. Anders, J. L. Beauchamp, R. C. Dunbar, and J. D. Baldeschwieler, *ibid.*, **45**, 1062 (1966).
(13) J. L. Beauchamp, L. R. Anders, and J. D. Baldeschwieler, *J. Am. Chem. Soc.*, **89**, 4569 (1967).
(14) J. D. Baldeschwieler, *Science*, **159**, 263 (1968).

the new method. Accordingly, this paper reports on the results of observations on CH_4–D_2 and CD_4–H_2 mixtures by this technique. In these experiments D_2 or H_2 served as stand-in for molecular tritium, and a beam of electrons caused the excitation and ionization instead of β particles and secondary electrons. The objectives of the present work were to map out in detail the complex sequences of competitive and consecutive ion–molecule reactions taking place when these gaseous mixtures are ionized, to determine some reaction rates in these mixtures, to compare our results with those found earlier in the high-pressure experiments, and to correlate the observations with the findings of conventional gas-phase kinetics studies, all in an effort to establish unambiguously the mechanisms important in the Wilzbach labeling of methane.

In brief summary of the principles underlying ion cyclotron resonance spectroscopy, a charged particle in a uniform magnetic field of magnitude H is constrained in its motion to a circular orbit in a plane normal to H, but is unrestricted in its motion parallel to H. The frequency of motion of the ion in its orbit, its cyclotron frequency ω_c, is given (in cgs units) by $\omega_c = q\mathbf{H}/Mc$, where q and M are the ionic charge and mass of the ion, respectively, and c is the velocity of light. If an alternating field E_1 of frequency ω_1 equal to the cyclotron frequency is applied in a direction normal to the magnetic field, the ion will absorb energy from the imposed electric field, and this absorption of energy can be detected by a sensitive marginal oscillator detector. Accordingly, the density of the ions of mass M in the combined magnetic–electric field can be measured, and since M varies linearly with H at fixed ω_c, the instrument becomes a mass spectrometer by simply varying the magnetic field to bring each ionic species in turn in resonance with the imposed electric field. The foregoing is then the basis of "ion cyclotron single resonance spectroscopy."

The power of the method for the study of ion chemistry becomes evident when the concentration of the gas in the cell within the magnetic field is great enough that collisions are possible. If we consider the generalized reaction $A^+ + B \rightarrow C^+ + D$, both A^+ and C^+ may be detected by the oscillator detector. Consider the situation where E_1 of frequency corresponding to ω_c of C^+ is applied and the absorption of energy is observed. Now if a second alternating electric field E_2 of frequency ω_2 equal to ω_c of A^+ is introduced, the reacting species will absorb energy, and its velocity and therefore its circular orbit will increase. The "heating" of the ion A^+ causes a significant change in its rate of reaction with B to form C^+ and D, and the change in concentration of C^+ will be directly recorded by the marginal oscillator detector, which has been set to observe C^+. Thus the reactant A^+ and the product C^+ of the reaction are definitely established. In similar manner, all the ions taking part in chains of consecutive reactions or in competitive reactions can be delineated. The new approach, consequently, avoids the uncertainty as to which of several possible species are participants in complex chains of ion–molecule reactions, a difficulty often occurring in "high-pressure" mass spectrometry. Additional advantages of "double or multiple icr" are the great sensitivity of the instrument for observing ion–molecule reactions, due to the very long ion paths in the cell, the absence of or greatly reduced mass discrimination effects inherent in conventional mass spectrometers, and the conservation of precious material because of the *in situ* nature of the experiment. The new approach has already been used in a wide variety of investigations of ion–molecule reactions.[12-23]

Experimental Section

The spectrometer used in the investigations reported here is the Varian Associates (Palo Alto, Calif.) Model V-5900 Syrotron. Descriptions of the machine have been adequately presented.[13] However, for the purposes of these experiments, an all-stainless steel, dual gas handling and inlet system was constructed, which contained reservoirs, variable leaks, and capacitance manometers (Granville-Phillips Co., Boulder, Colo.). This inlet system enabled us to control independently the pressures of two kinds of gases in the resonance cell between 10^{-6} and 10^{-3} Torr.

The single resonance experiments were performed either by modulating the magnetic field or by modulating the source drift potential. All the double resonance studies reported here were carried out by applying the output of the double resonance oscillator to the source region of the cell and sweeping the frequency of this oscillator. The intensity of the ionizing electron beam was kept lower than 0.20 μA and controlled by a Mosfet electrometer in order to minimize undesirable space charge effects in the relatively high-pressure experiments. The sample pressure in the cell was determined from measurements of the total positive ion current arriving at the ion collector at the end of the cell, the ionizing electron beam current and path length, and the literature values of the total ionization cross section of the sample molecule.

Each of the reagent gases, 99.9% methane (Phillips Petroleum Co.), 99.5% deuterium (Air Products & Chemicals, Inc.), 99% isotopically pure CD_4 (Merck Sharp & Dohme of Canada, Ltd.), and nitric oxide (Technical Grade (98.5%) from Matheson Co.) were further purified with molecular sieve or with activated charcoal at liquid nitrogen temperature. High-purity xenon (99.995%) and hydrogen (99.9995%) obtained from Air Reduction Corp. were used without further purification.

Results

1. Single Resonance Spectra. Figure 1 shows the single resonance icr spectra of two different $CH_4 + D_2$ mixtures in comparison with the mass spectrum of pure methane, all being measured at the same partial pressure of CH_4. The experimental conditions were: energy of ionizing electrons = 70 eV, drift voltage = 95 mV/cm, observing oscillator frequency = 306 kc/sec, radiofrequency power level = 145 mV/cm. The instrument was operated in the pulsed drift modulation mode. The mass spectrum of pure methane at the source pressure of 4.55×10^{-5} Torr is seen to include the primary positive ions from CH_4 as well as several products of ion–molecule reactions, particularly the prominent CH_5^+ and $C_2H_5^+$ species. But as deuterium gas is added in increasing amounts, the intensities of many of these ions, *e.g.*, those of mass to charge (m/e) ratio 12, 13, 14, 15, 26, 27, 28, and 29, decrease, and the abundances of many others, notably of m/e 4, 6, 16, 17, 18, 30, 31, and 32, remain the same or increase. The former group has been assigned the formulas C^+, CH^+, CH_2^+, CH_3^+, $C_2H_2^+$, $C_2H_3^+$, $C_2H_4^+$, and $C_2H_5^+$, respectively, and the latter mass group to D_2^+, D_3^+, CH_2D^+ +

(15) J. L. Beauchamp, *J. Chem. Phys.*, 46, 1231 (1967).
(16) J. M. S. Henis, *J. Am. Chem. Soc.*, 90, 844 (1968).
(17) J. L. Beauchamp and S. E. Buttrill, Jr., *J. Chem. Phys.*, 48, 1783 (1968).
(18) M. T. Bowers, D. D. Elleman, and J. L. Beauchamp, *J. Phys. Chem.*, 72, 3599 (1968).
(19) G. A. Gray, *J. Am. Chem. Soc.*, 90, 2177, 6002 (1968).
(20) R. C. Dunbar, *ibid.*, 90, 5676 (1968).
(21) J. King, Jr., and D. D. Elleman, *J. Chem. Phys.*, 48, 412 (1968).
(22) J. I. Brauman and L. K. Blair, *J. Am. Chem. Soc.*, 90, 5636, 6561 (1968).
(23) F. Kaplan, *ibid.*, 90, 4483 (1968).

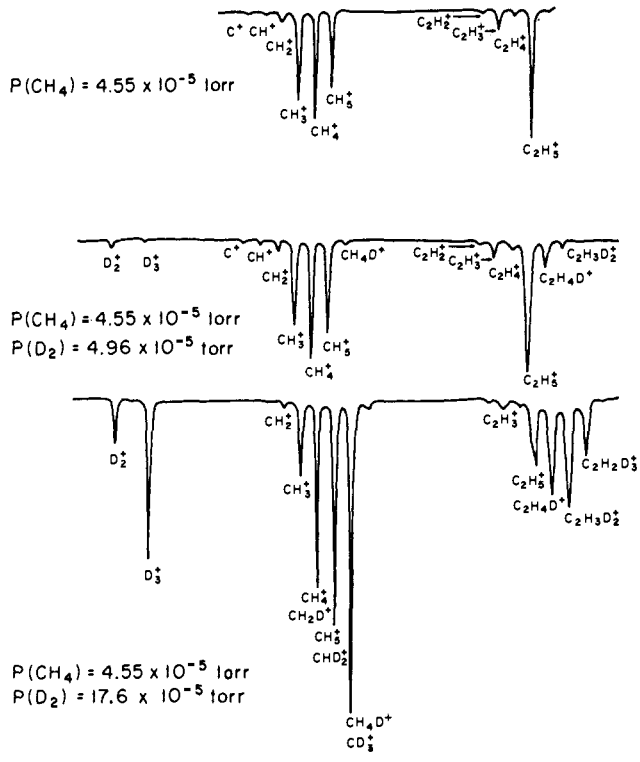

Figure 1. Single resonance spectra of CH_4 and of $CH_4 + D_2$ mixtures observed by pulsed drift modulation technique.

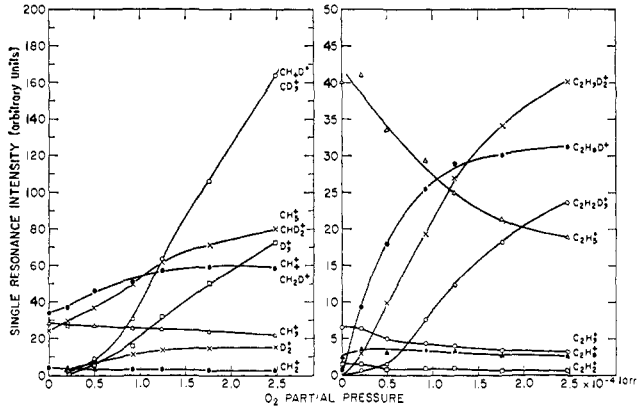

Figure 2. Dependence of single resonance signals of ions on pressure of D_2 in the Syrotron cell. The pressure of CH_4 was 2.7×10^{-5} Torr; pulsed drift modulation was employed; the energy of the electron ionizing current was 70 V.

CH_4^+, $CH_5^+ + CHD_2^+$, $CH_4D^+ + CD_3^+$, $C_2H_4D^+$, $C_2H_3D_2^+$, and $C_2H_2D_3^+$, respectively. The behavior of the mass spectra of ions in these mixtures, as one may observe from the plots in Figure 2, is similar to that found with the "high-pressure" mass spectrometric technique.[9,10] Here the single resonance intensities of virtually all ions of interest have been plotted as a function of increasing partial pressure of D_2 and fixed pressure of CH_4. The yield of D_2^+ initially increases but then levels off as that of D_3^+ rises rapidly. The intensities of CH_2^+ and CH_3^+ remain fairly insensitive to added D_2, but the functions for deuterated single carbon-containing ions such as CHD_2^+, CH_4D^+, and CD_3^+ increase greatly. Even more contrasting behaviors are shown by the ethyl ions. Although $C_2H_5^+$ decreases exponentially, the three deuterated species rise greatly as the pressure of

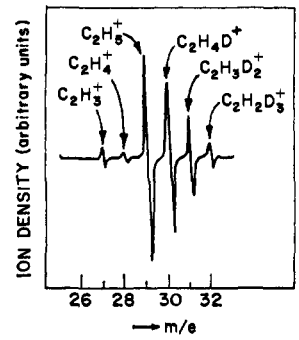

Figure 3. Partial single resonance spectrum of $D_2 + CH_4$ system obtained by sweeping the magnetic field.

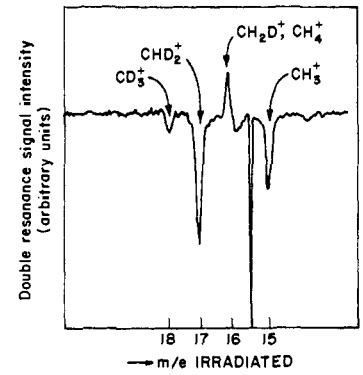

Figure 4. Double resonance spectrum of $C_2H_3D_2^+$ observed ion.

D_2 is increased. From the shapes of the latter three curves, one may conclude that the dependence of yield of $C_2H_4D^+$ on concentration of D_2 is at least first order, of $C_2H_3D_2^+$ second order, and of $C_2H_2D_3^+$ third order. Similar behaviors were observed for the equivalent ions in CD_4–H_2 gaseous mixtures as functions of the hydrogen partial pressure. From comparison of the absolute yields of CH_3^+ and CD_4H^+ in the latter mixtures, however, we conclude that the curve in Figure 2 representing the sum of $CH_4D^+ + CD_3^+$ is preponderantly (~85%) the behavior of the CH_4D^+ species. Similarly, about 75% of the ions showing the characteristics of the curve denoted by CH_5^+ and CHD_2^+ are the former species. Indeed, the intensity of the CHD_2^+ species in CD_4–H_2 mixtures rises to a maximum and then decreases, CDH_2^+ grows to a maximum, CH_3^+ is continuously and rapidly increasing, and CD_3^+ decreases exponentially, as the pressure of H_2 is raised from 0 to 3.0×10^{-4} Torr. In addition, the curve for CD_4H^+ rises rapidly and linearly, while those for CD_4^+ and CD_5^+ increase slightly and then level off.

A partial spectrum for the mass range from 26 to 32 obtained by varying the magnetic field appears in Figure 3. Magnetic field modulation causes the observed derivative line shape.

2. Double Resonance Spectra. The Mechanisms of Isotopic Exchange. Typical of the observations when the instrument is operated in the double resonance mode is the partial spectrum presented in Figure 4. Here the $C_2H_3D_2^+$ ion was observed by the marginal oscillator-detector, and the frequency of the second alternating electric field was varied to bring into resonance each of the other ionic species. A signal appears when the species at resonance is a reactant that produces the $C_2H_3D_2^+$

ion. Note that the direction of the double resonance signal is negative for the ions CD_3^+, CHD_2^+, and CH_3^+, but positive for $CH_2D^+ + CH_4^+$. The sharp spike at *m/e* 15.5 is due to the irradiating oscillator exciting the first overtone of the marginal oscillator, which had been set to observe the species of *m/e* 31. Table I contains a compilation of all combinations of reactant and product species exhibiting a double resonance signal in $CH_4 + D_2$ mixtures. The ions are arranged in columns of species observed (mass number and probable formula) and species irradiated. From these data and stoichiometric considerations, the many sequences of competitive and consecutive ion–molecule reactions that take place in the gas may be mapped out in stepwise fashion. Thus, for the ion CH_3^+ observed as the product, we may write the reactions listed adjacent to this species in column 5. Note that the CH_3^+ is formed by collisional dissociation of CH_5^+ and CH_4D^+, in addition to being a primary species from electron impact ionization of the methane. The products of mass 16 must be CH_4^+ and CH_2D^+, and the double resonance data obtained for this mass are combined with information previously gained for the CH_3^+ ion to arrive at the modes of reaction shown for mass 16 in column 5. It is seen that CH_4^+ is formed as a product from reaction of CH_3^+ with methane, while CH_2D^+ is produced in separate reactions by D_3^+, CH_4D^+, and CH_3^+. This procedure of building onto previously established ionic sequences reactions indicated by double resonance pairings of reactant and product species is continued, in order, for species of masses 17, 18, 29, 30, 31, and 32. As shown in the table, the mechanisms of ion–molecule reactions become more complex.

The only ambiguities apparent at this stage of the work were due to overlap of different ions of the same mass. Thus, mass 16 could be assigned to CH_4^+ and CH_2D^+, mass 17 to CH_5^+ and CHD_2^+, and mass 18 to CH_4D^+ and CD_3^+. These difficulties were overcome by investigations on the isotopically inverse system $CD_4 + H_2$. For then the CD_4^+ ion (mass 20), equivalent to CH_4^+ in the $CH_4 + D_2$ mixtures, is greater in mass than CHD_2^+ (mass 17), CD_5^+ greater than CDH_2^+, and CD_4H^+ greater than CH_3^+. The results of double resonance studies on the deuterated methane plus hydrogen mixtures are assembled in Table II. The elimination of ambiguity over which of the two possible reactant ions of masses 16, 17, and 18, respectively, is responsible for certain reactions outlined in Table I is illustrated by the data for the observed ion CHD_2^+ in the former table. Note that double resonance signals in the CD_4–H_2 mixtures are observed for CD_3^+, CD_4^+, CD_4H^+, and CD_5^+ reactants, but not for CDH_2^+ and CH_3^+. Consequently, in $CH_4 + D_2$ mixtures the irradiated reactant ions giving CH_2D^+ as an eventual product are CH_3^+, CH_4^+, CH_4D^+, and CH_5^+, but could not be CHD_2^+ and CD_3^+, respectively. Similar correlations of the data serve to remove doubts of the identities of the ions in the other sequences of reactions presented in Table I.

All the separate sequences of ionic reactions in the $CH_4 + D_2$ system (Table I) have been combined to give in Figure 5 the competitive and consecutive modes by which hydrogen atoms in organic fragments are replaced by deuterium. A number of characteristics of this isotopic exchange are evident.

(a) Reactions in which deuterium atoms become incorporated in carbon-containing species are initiated by

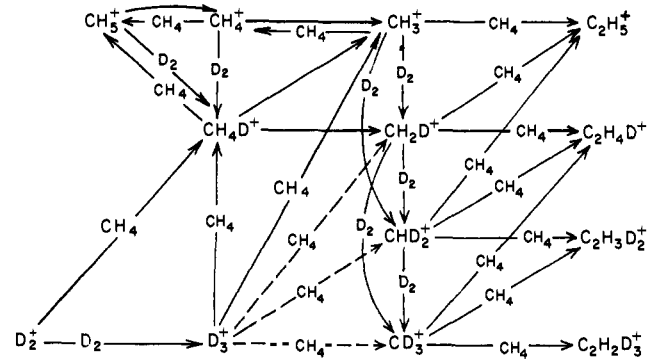

Figure 5. Mechanisms of isotopic exchange of hydrogen and deuterium atoms in D_2–CH_4 gaseous mixtures.

reactant ions from both CH_4 and D_2. In illustration, CH_4D^+ may be formed from CH_4^+ and CH_5^+ and from D_2^+ and D_3^+.

(b) Purely isotopic exchange occurs in reactions of methyl ions (CH_3^+, CH_2D^+, and CHD_2^+) with deuterium molecules. Reactions in which two atoms of hydrogen are replaced occur in competition with those collisions where only one hydrogen atom is exchanged for deuterium. Consecutive reactions lead to the fully deuterated methyl species.

(c) Deuterated methyl ions are formed by the additional mechanisms of unimolecular and collisional dissociation of CH_4D^+. These modes of reaction probably occur for CH_4D^+ even at thermal energies, because the amount of energy with which it is formed from D_2^+ or D_3^+ is more than sufficient to overcome the endothermicity of the dissociation (see Table III below). Furthermore, negative double resonance signals are observed for D_2^+ and D_3^+ and the deuterated methyl species. Although such signals were observed for D_3^+ and CH_2D^+, CHD_2^+, and CD_3^+, respectively, it is unlikely that D_3^+ reacts with CH_4 to form a $CH_4D_3^+$ complex required to yield the deuterated methyl ions. It is more plausible that CH_4D^+ is first formed, and the methyl species are formed in consecutive reactions which follow formation of this ion. Accordingly, the dashed arrows in Figure 5 indicate that double resonance signals were observed between the indicated pairs, but that direct reactions are not likely.

(d) The CH_3^+ and isotopically labeled methyl ions combine with CH_4 to yield ethyl ions in which none, one, two, or three of its hydrogens are replaced by deuterium atoms. The ethyl ions do not react further with D_2 to produce more fully deuterated products, in contrast to the behavior of the methyl moieties. Furthermore, the ethyl species are relatively inert toward methane since ionic products containing three or more carbon atoms were found in very small yields.

(e) The secondary species CH_5^+ exchanges atoms with D_2 to give CH_4D^+ and the latter can re-form the former by exchange of hydrogen and deuterium atoms in a collision with a CH_4 molecule. The first exchange reaction probably proceeds through a very short-lived ion-induced dipole transient CH_5^+–D_2 in which a H atom and a D atom exchange places rapidly, rather than through a long-lived intermediate consisting of a $CH_5D_2^+$-collision complex with classical valence bonds.

3. Effect of Amplitude of Irradiation Field. Types of Ionic Reactions Taking Place in the Gas-

Table I. Double Resonance Spectra of Secondary Ions in $D_2 + CH_4$ Mixtures

Species observed m/e	Ion	Species irradiated m/e	Ion	Probable reaction mechanisms
15	CH_3^+	4	D_2^+	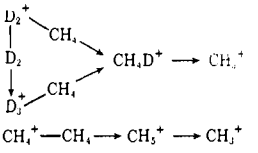
		6	D_3^+	
		16	CH_4^+	
		17	CH_5^+	
		18	CH_4D^+	
16	CH_4^+	4	D_2^+	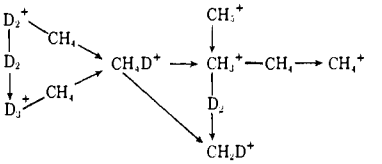
	CH_2D^+	6	D_3^+	
		15	CH_3^+	
		17	CH_5^+	
		18	CH_4D^+	
17	CH_5^+	4	D_2^+	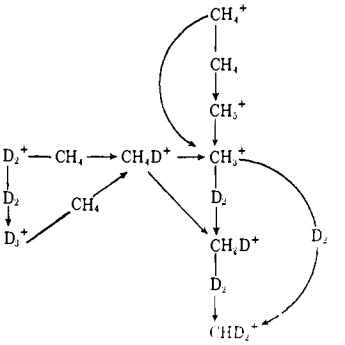
	CHD_2^+	6	D_3^+	
		14	CH_2^+	
		15	CH_3^+	
		16	CH_4^+	
			CH_2D^+	
		18	CH_4D^+	
18	CH_4D^+	4	D_2^+	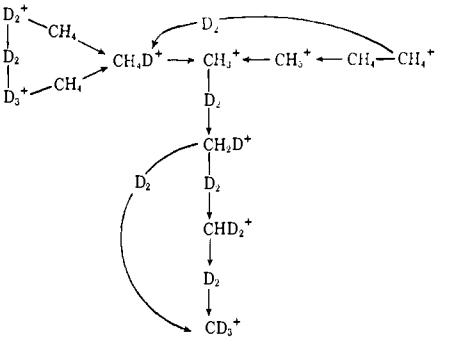
	CD_3^+	6	D_3^+	
		15	CH_3^+	
		16	CH_4^+	
			CH_2D^+	
		17	CH_5^+	
			CHD_2^+	
29	$C_2H_5^+$	4	D_2^+	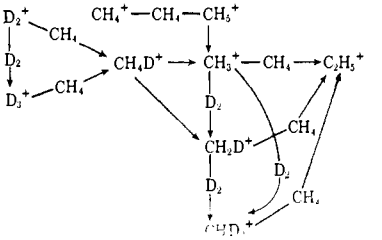
		6	D_3^+	
		14	CH_2^+	
		15	CH_3^+	
		16	CH_4^+	
			CH_2D^+	
		17	CH_5^+,	
			CHD_2^+	
		18	CH_4D^+	
30	$C_2H_4D^+$	4	D_2^+	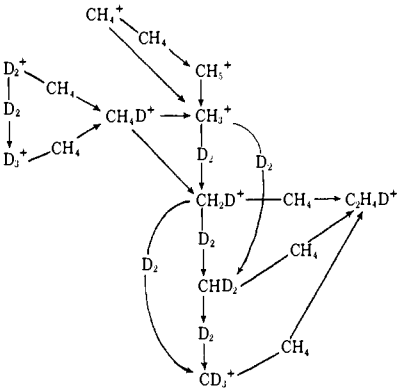
		6	D_3^+	
		14	CH_2^+	
		15	CH_3^+	
		16	CH_4^+	
			CH_2D^+	
		17	CH_5^+	
			CHD_2^+	
		18	CH_4D^+	
			CD_3^+	

Table I (*Continued*)

Species observed m/e	Ion	Species irradiated m/e	Ion	Probable reaction mechanisms
31	$C_2H_3D_2^+$	4	D_2^+	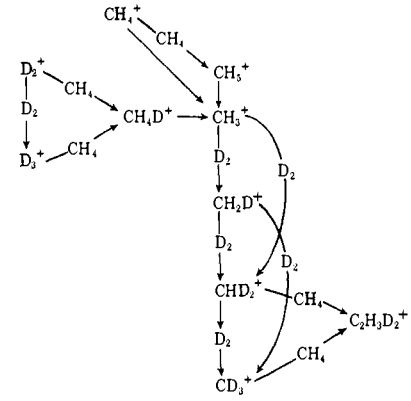
		6	D_3^+	
		14	CH_2^+	
		15	CH_3^+	
		16	CH_4^+	
			CH_2D^+	
		17	CH_5^+	
			CHD_2^+	
		18	CH_4D^+	
			CD_3^+	
32	$C_2H_2D_3^+$	4	D_2^+	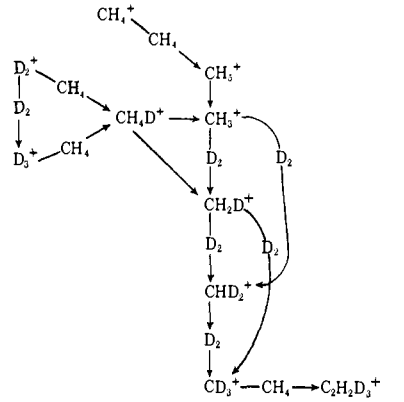
		6	D_3^+	
		14	CH_2^+	
		15	CH_3^+	
		16	CH_4^+	
			CH_2D^+	
		17	CH_5^+	
			CHD_2^+	
		18	CH_4D^+	
			CD_3^+	

eous Systems. Since the direction of the double resonance signal relative to single resonance is an indication of the sign of the over-all change in rate constants with increased ion energy of the particular ion–molecule reactions leading to the product being observed, and the sign may in many cases establish the kinds of ionic reactions taking place, a systematic study was made of the variation of the double resonance signal with the power of the irradiating electric field. In illustration, Figure 6 gives the results obtained when the signal for the $C_2H_4D^+$ ion was observed as a function of the absorbed energy A_{rf} (which is proportional to the square of the radiofrequency electric field, E_{rf}^2) of the irradiating field that "heated" in turn the several reactant ions shown in the figure. From plots such as these, the directions of the initial rate of change of reaction rate with radiofrequency power, $dk/dA_{rf} = dk/dE_{ion}$ where E_{ion} is the ion energy, were obtained for the ionic reactions listed in Table III. The appropriate heats of reaction $\Delta H^{298°K}$ are also included. It is apparent from the table that an initial positive slope of dk/dE_{ion} corresponds to an endothermic reaction, while a negative slope indicates that the ionic reaction is exoergic, thermoneutral, or, in two cases, endoergic if the ions in the latter are assumed to be in their ground states. Note that in the gaseous mixtures studied here, only collisional dissociations of CH_5^+- and CH_4^+-like ions are endoergic, all the others being either exoergic or thermoneutral. The negative double resonance signals observed for the former reactions are probably indicative of the CH_4^+, CH_5^+, and CH_4D^+ being formed as vibrationally excited species.

For consecutive reactions, however, the over-all behavior of the slope is the sum of the individual effects on the reaction rates. Thus in Figure 6 the initial rise of

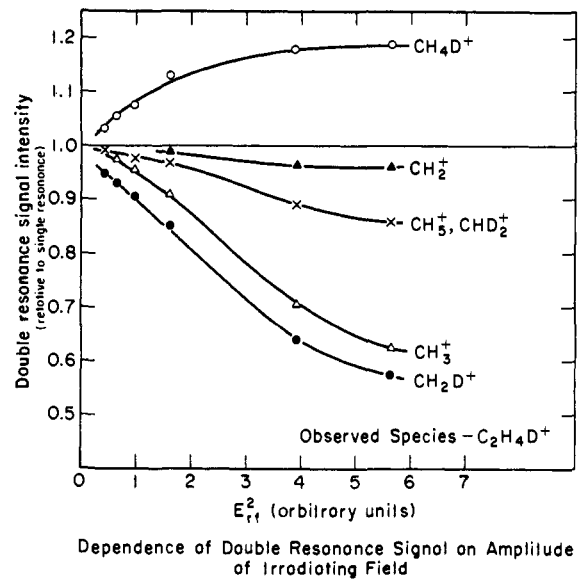

Dependence of Double Resonance Signal on Amplitude of Irradiating Field

Figure 6. Dependence of double resonance signal on amplitude of irradiating radiofrequency field.

the double resonance signal with increasing radiofrequency power suggests that here the $C_2H_4D^+$ is being formed by collisional dissociation of CH_4D^+ to CH_2D^+

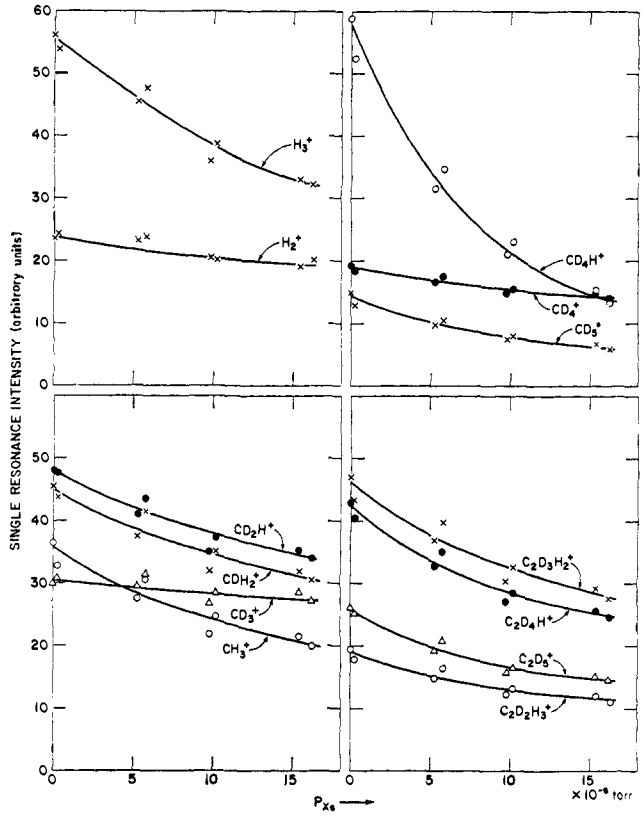

Figure 7. Effect of Xe on single resonance signals of species in a CD_4–H_2 mixture. The pressures of CD_4 and H_2 were 0.92×10^{-5} and 7.0×10^{-5} Torr, respectively.

followed by the latter's condensation reaction with a CH_4 molecule. The higher rate of dissociation of CH_4D^+ as its velocity is increased apparently more than balances the lower rate of the condensation reaction. On the other hand, the initial slope of the double resonance signal for mass 30 observed — mass 15 irradiated is negative, because the two successive reactions

$$CH_3^+ + D_2 \longrightarrow CH_2D^+ + HD \quad (1)$$

$$CH_2D^+ + CH_4 \longrightarrow C_2H_4D^+ + H_2 \quad (2)$$

are thermoneutral and exoergic, respectively. Similarly, the direction of the curve denoted by CH_2D^+ suggests the exoergic reaction 2, but the negative slope of the curve marked CH_5^+ and CHD_2^+ is much less than those for the two methyl ions just discussed. It is likely that this curve represents the over-all effect of increasing radiofrequency power absorption on several reactions, probably reactions 1 and 2 and

$$CH_5^+ \longrightarrow CH_3^+ + H_2 \quad (3)$$

$$CH_3^+ + D_2 \longrightarrow CHD_2^+ + H_2 \quad (4)$$

$$CHD_2^+ + CH_4 \longrightarrow C_2H_4D^+ + HD \quad (5)$$

Raising the amplitude of absorption will increase the rate of reaction 3, which will partially compensate for the lower rates of the other reactions. Similar partial cancellations of the effects of radiofrequency power absorption were observed in many of the double resonance experiments.

4. Effects of Xenon and Nitric Oxide. The variations, with increasing xenon concentration, of the single resonance intensities of all the ionic species of interest are illustrated by the data for a CD_4–H_2 mixture presented in Figure 7. In this experiment the partial pressures of CD_4 and H_2 were 0.92×10^{-5} and 7.0×10^{-5} Torr, respectively, and the Xe pressure was increased in the range from 0 to 1.5×10^{-5} Torr. Study of the figure reveals that the presence of Xe strongly depresses the intensities of H_3^+, CD_5^+, and CD_4H^+, but the rare gas has little effect on H_2^+, CD_4^+, and CD_3^+. Note that the intensity of CD_4H^+ decreases by a much greater percentage than that of D_3^+ from which it is in part formed. Similar effects were observed when xenon was added stepwise to a CH_4–D_2 mixture. Furthermore, double resonance studies of a CH_4–D_2 mixture with increasing

Table II. Double Resonance Spectra of the CD_4–H_2 System

Observed ion m/e	Observed ion	Irradiated ion m/e	Irradiated ion	Double resonance signal intensity[a]
15	CH_5^+	3	H_3^+	
		16	CDH_2^+	−15.4
		17	CD_2H^+	−21.6
		18	CD_3^+	−36.2
		20	CD_4^+	+15.4
		21	CD_4H^+	+16.1
		22	CD_5^+	+16.9
16	CH_2D^+	17	CD_2H^+	−23.6
		18	CD_3^+	−40.5
		20	CD_4^+	−5.4
		21	CD_4H^+	−11.2
		22	CD_5^+	−11.8
17	CHD_2^+	18	CD_3^+	−26.7
		20	CD_4^+	−11.5
		21	CD_4H^+	−4.6
		22	CD_5^+	−4.9
18	CD_3^+	20	CD_4^+	−9.5
		21	CD_4H^+	−5.2
		22	CD_5^+	−9.5
20	CD_4^+	18	CD_3^+	−4.1
		21	CD_4H^+	+6.6
		22	CD_5^+	+5.7
21	CD_4H^+	20	CD_4^+	−49.5
		22	CD_5^+	−27.5
22	CD_5^+	20	CD_4^+	−66.1
		21	CD_4H^+	−8.7
34	$C_2D_5^+$	15	CH_3^+	+3.26
		16	CDH_2^+	+3.70
		17	CD_2H^+	−4.45
		18	CD_3^+	−15.0
		20	CD_4^+	+14.1
		21	CD_4H^+	+20.0
		22	CD_5^+	+42.2
33	$C_2D_4H^+$	16	CDH_2^+	−11.5
		17	CD_2H^+	−20.5
		18	CD_3^+	−11.1
		20	CD_4^+	+13.7
		21	CD_4H^+	+20.8
		22	CD_5^+	−41.0
32	$C_2D_3H_2^+$	15	CH_3^+	−15.8
		16	CH_2D^+	−24.8
		17	CHD_2^+	−10.8
		18	CD_3^+	−7.7
		20	CD_4^+	+13.5
		21	CD_4H^+	+21.4
		22	CD_5^+	+43.5
31	$C_2D_2H_3^+$	15	CH_3^+	−35.0
		16	CH_2D^+	−21.4
		17	CHD_2^+	−12.6
		18	CD_3^+	−8.7
		20	CD_4^+	+15.5
		21	CD_4H^+	+21.8
		22	CD_5^+	+48.5

[a] % of the single resonance intensity of observed ion. The sign indicates the direction of the double resonance signal relative to the intensity of the single resonance.

Table III. Relation between $\Delta H_{reaction}$ and Sign of $(dk/dE_{ion})^0$

Reaction	$\Delta H_{reaction}$, kcal/mole	Double resonance signal observed	Sign of $(dk/dE_{ion})^0$
$D_2^+ + CH_4 \rightarrow CH_4D^+ + D$	$54 < \Delta H < 60$	$D(4 \rightarrow 18)$	−
$D_3^+ + CH_4 \rightarrow CH_4D^+ + D_2$	$30 < \Delta H < 60$	$D(6 \rightarrow 18)$	−
$D_3^+ + CH_4 \rightarrow CHD_2^+ + HD + H_2$	$0 < \Delta H < 24$	$D(6 \rightarrow 17)$	−
$CH_3^+ + CH_4 \rightarrow C_2H_5^+ + H_2$	$20 < \Delta H < 24$	$D(15 \rightarrow 29)$	−
$CH_3^+ + D_2 \rightarrow CH_2D^+ + HD$	Neutral	$D(15 \rightarrow 16)$	−
$CH_2D^+ + CH_4 \rightarrow C_2H_4D^+ + H_2$	$20 < \Delta H < 24$	$D(16 \rightarrow 30)$	−
$CDH_2^+ + H_2 \rightarrow CH_3^+ + HD$	Neutral	$D(16 \rightarrow 15)^b$	−
$CHD_2^+ + CH_4 \rightarrow C_2H_3D_2^+ + H_2$	$20 < \Delta H < 24$	$D(17 \rightarrow 31)$	−
$CD_2H^+ + H_2 \rightarrow CDH_2^+ + HD$	Neutral	$D(17 \rightarrow 16)^b$	−
$\searrow CH_3^+ + D_2$	Neutral	$D(17 \rightarrow 15)^b$	−
$CD_3^+ + CH_4 \rightarrow C_2H_3D_2^+ + HD$	$20 < \Delta H < 24$	$D(18 \rightarrow 31)$	−
$CD_3^+ + CH_4 \rightarrow C_2H_2D_3^+ + H_2$	$20 < \Delta H < 24$	$D(18 \rightarrow 32)$	−
$CD_3^+ + H_2 \rightarrow CD_2H^+ + HD$	Neutral	$D(18 \rightarrow 17)^b$	−
$\searrow CDH_2^+ + D_2$	Neutral	$D(18 \rightarrow 16)^b$	−
$CH_4^+ + CH_4 \rightarrow CH_5^+ + CH_3$	$4 < \Delta H < 10$	$D(16 \rightarrow 17)$	−
$CH_4^+ + D_2 \rightarrow CH_4D^+ + D$	$1 < \Delta H < 7$	$D(16 \rightarrow 18)$	−
$CH_4^+ \rightarrow CH_3^+ + H$	-29^a	$D(16 \rightarrow 15)$	+ or −
$CH_5^+ \rightarrow CH_4^+ + H$	$-111^a < \Delta H < -105^a$	$D(17 \rightarrow 16)$	+ or −
$CH_5^+ \rightarrow CH_3^+ + H_2$	$-36^a < \Delta H < -30^a$	$D(17 \rightarrow 15)$	+
$CH_5^+ + D_2 \rightarrow CH_4D^+ + HD$	Neutral	$D[17 \rightarrow 18)$	−
$CH_4D^+ \rightarrow CH_2D^+ + H_2$	$-36^a < \Delta H < -30^a$	$D(18 \rightarrow 16)$	+
$CH_4D^+ + CH_4 \rightarrow CH_5^+ + CH_3D$	Neutral	$D(18 \rightarrow 17)$	−

[a] It is assumed that the reactant ion is not in an excited state. [b] The reaction in the $CD_4 + H_2$ system was studied.

partial pressures of Xe confirmed that D_3^+, CH_4D^+, and CH_5^+ were efficiently quenched by charge and proton transfer, while CH_3^+ was relatively inert toward the rare gas, and the results of a similar investigation on the inverse system CD_4–H_2 showed that the intensities of the various methyl species were relatively insensitive to Xe. We may conclude from these results that xenon quenches the species D_3^+, CH_5^+, and CH_4D^+ in CH_4–D_2 mixtures, and consequently inhibits all the reactions of these species shown in Figure 5. As a consequence, the sequences of ion-molecule reactions initiated by these ions and ending in the isotopically labeled ethyl ions should be eliminated by xenon. However, since Xe has virtually no effect on CD_3^+ (Figure 7), the production of deuterated ethyl ions following the chains of reactions beginning with CH_3^+ (Figure 5) should be unaffected. The lowerings of yields of hydrogenated methyls and ethyls with added xenon merely reflect the quenched contributions of H_3^+, CD_4H^+, and CH_5^+ reactants to their formations. In all cases the decrease of abundance is less than that for the three initially affected ions.

The addition of nitric oxide to mixtures of CD_4 and H_2 provoked changes in abundances of the various species similar to those caused by adding xenon. Thus, H_2^+, H_3^+, CD_4H^+, and CD_5^+ were greatly reduced, while the yield of CD_3^+ was only slightly lowered. Intermediate in behavior were the species CD_2H^+, CDH_2^+, and CH_3^+ among the methyl ions and $C_2D_5^+$, $C_2D_4H^+$, and $C_2D_3H_2^+$ of the ethyl-like products, but difficulties occurred in the interpretation of the behaviors of other species because of interference from charged species originating from the added nitric oxide. Then the peak at mass 31 increased with NO concentration, probably as a result of formation of NOH^+ by proton transfer reactions, and the yield of NO^+ (mass 30) also rose. Double resonance studies showed that all the methyl species in addition to CD_4H^+ and CD_5^+ exchanged charge with nitric oxide.

Determination of Rate Constants of Reactions

Reactions of ions produced by low-energy electrons (13.1 eV [AP(CH_4^+)] < E_e < 14.4 eV [AP(CH_3^+)]) were studied in the $CH_4 + D_2$ system, under which condition only the ions CH_4^+, CH_5^+, and CH_4D^+ were found in the mass spectrum. The rate constants k_1 and k_2 of the reactions

$$CH_4^+ + CH_4 \xrightarrow{k_1} CH_5^+ + CH_3 \quad (6)$$

$$CH_4^+ + D_2 \xrightarrow{k_2} CH_4D^+ + D \quad (7)$$

were determined by the method developed by Bowers, *et al.*,[18] but extended to this binary system in the following manner.

If $P(t)$ is the CH_4^+ ion current, $P(0)$ is the rate of formation of the CH_4^+ ions at the position of the electron beam in the source (at time $t = 0$), and $S_1(t)$ and $S_2(t)$ are the respective ion currents of CH_5^+ and CH_4D^+ produced by reactions 6 and 7 at time t, then

$$\frac{dP}{dt} = -(n_1k_1 + n_2k_2)P(t) \quad (8)$$

$$\frac{dS_1}{dt} = n_1k_1P(t) \quad (9)$$

$$\frac{dS_2}{dt} = n_2k_2P(t) \quad (10)$$

where n_1 and n_2 are the concentrations of the reactant molecules CH_4 and D_2, respectively. The solutions of eq 8, 9, and 10 are

$$P(t) = P(0)\exp\{-(n_1k_1 + n_2k_2)t\} \quad (11)$$

$$S_1(t) = \frac{n_1k_1}{n_1k_1 + n_2k_2} \times P(0)[1 - \exp\{-(n_1k_1 + n_2k_2)t\}] \quad (12)$$

$$S_2(t) = \frac{n_2k_2}{n_1k_1 + n_2k_2} \times P(0)[1 - \exp\{-(n_1k_1 + n_2k_2)t\}] \quad (13)$$

The observed single resonance intensities I_p, I_{s_1}, and I_{s_2} of the primary and secondary ions are obtained by integrating $P(t)$, $S_1(t)$, and $S_2(t)$ over the time the ion

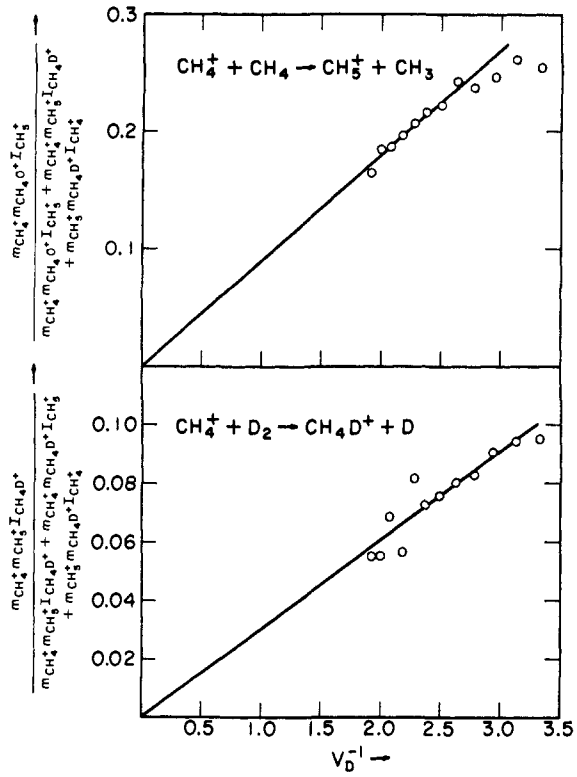

Figure 8. Plots of functions of ion intensities *vs.* the reciprocal of the drift voltage, V_D^{-1}. Rate constants for the two reactions denoted in the figure are obtained from the slopes of the curves by the method described in the text.

spends in the analyzer region of the cell of the Syrotron (t to t' where t and t' are the times at which the ion enters and leaves the analyzer region), multiplying by the factors $C_p/m_p = e^2E_1^2/4m_p\xi_p$, $C_{s_1}/m_{s_1} = e^2E_1^2/4m_{s_1}\xi_{s_1}$, and $C_{s_2}/m_{s_2} = e^2E_1^2/4m_{s_2}\xi_{s_2}$, respectively, which arise from the expression for the power absorption by the ions.[15] Here E_1 is the radio frequency electric field strength, m_p, m_{s_1}, and m_{s_2} are the respective masses of the primary and secondary ions, ξ_{p_1}, ξ_{s_1}, and ξ_{s_2} are the appropriate collision frequencies for momentum transfer, and the C's are the functions defined above. Thus

$$I_p = \frac{C_p}{m_p}\int_{t_p}^{t_p'} P(t)\mathrm{d}t = \frac{C_pP(0)}{m_p(n_1k_1 + n_2k_2)} \times [\exp\{-(n_1k_1 + n_2k_2)t_p\} - \exp\{-(n_1k_1 + n_2k_2)t_p'\}] \quad (14)$$

$$I_{s_1} = \frac{C_{s_1}P(0)n_1k_1}{m_{s_1}(n_1k_1 + n_2k_2)^2}[(n_1k_1 + n_2k_2)(t_{s_1}' - t_{s_1}) + \exp\{-(n_1k_1 + n_2k_2)t_{s_1}'\} - \exp\{-(n_1k_1 + n_2k_2)t_{s_1}\}] \quad (15)$$

$$I_{s_2} = \frac{C_{s_1}P(0)n_2k_2}{m_{s_2}(n_1k_1 + n_2k_2)^2}[(n_1k_1 + n_2k_2)(t_{s_2}' - t_{s_2}) + \exp\{-(n_1k_1 + n_2k_2)t_{s_2}'\} - \exp\{-(n_1k_1 + n_2k_2)t_{s_2}\}] \quad (16)$$

If $(n_1k_1 + n_2k_2)t_p \ll 1$, $(n_1k_1 + n_2k_2)t_p' \ll 1$, etc., eq 14, 15, and 16 may be expanded to give

$$I_p \simeq \frac{C_pP(0)}{m_p}(t_p' - t_p) \times \{1 - {}^1/_2(n_1k_1 + n_2k_2)(t_p' + t_p)\} \quad (17)$$

$$I_{s_1} \simeq \frac{C_{s_1}P(0)n_1k_1}{m_{s_1}}\frac{(t_{s_1}' - t_{s_1})(t_{s_1}' + t_{s_1})}{2} \quad (18)$$

$$I_{s_2} \simeq \frac{C_{s_2}P(0)n_2k_2}{m_{s_2}}\frac{(t_{s_2}' - t_{s_2})(t_{s_2}' + t_{s_2})}{2} \quad (19)$$

When the instrument is operated in the magnetic sweep mode, t and m are proportional to the magnetic field, so that t_{s_1}, t_{s_1}', t_{s_2}, and t_{s_2}' may be replaced by

$$t_{s_1} = \frac{m_{s_1}}{m_p}t_p;\ t_{s_1}' = \frac{m_{s_1}}{m_p}t_p';\ t_{s_2} = \frac{m_{s_2}}{m_p}t_p;\ t_{s_2}' = \frac{m_{s_2}}{m_p}t_p' \quad (20)$$

and eq 18 and 19 become

$$I_{s_1} = \frac{C_{s_1}P(0)n_1k_1m_{s_1}}{2m_p^2}(t_p' - t_p)(t_p' + t_p) \quad (21)$$

$$I_{s_2} = \frac{C_{s_2}P(0)n_2k_2m_{s_2}}{2m_p^2}(t_p' - t_p)(t_p' + t_p) \quad (22)$$

Solving eq 17, 21, and 22 for k_1 and k_2 gives

$$k_1 = \frac{2}{m_1(t_p' + t_p)} \times \frac{\xi_{s_1}I_{s_1}m_pm_{s_2}}{\xi_{s_1}I_{s_1}m_pm_{s_2} + \xi_pI_pm_{s_1}m_{s_2} + \xi_{s_2}I_{s_2}m_{s_1}m_p} \quad (23)$$

$$k_2 = \frac{2}{m_2(t_p' + t_p)} \times \frac{\xi_{s_2}I_{s_2}m_pm_{s_1}}{\xi_{s_1}I_{s_1}m_pm_{s_2} + \xi_pI_pm_{s_1}m_{s_2} + \xi_{s_2}I_{s_2}m_{s_1}m_p} \quad (24)$$

where the ratios $C_{s_1}/C_p = \xi_p/\xi_{s_1}$ and $C_{s_1}/C_{s_2} = \xi_{s_2}/\xi_{s_1}$ have been used to substitute ξ for C. In order to simplify the expressions for k and to correlate them with the experimental results, we assume that all the collision frequencies for momentum transfer are approximately equal.

Figure 8 shows plots of the complex fractions of eq 23 and 24 as functions of the inverse of the drift voltage, V_D^{-1}. The latter is related to t and t' by

$$t = Hdl_1/V_D, \quad t' = Hdl_2/V_D$$

where H is the magnetic field strength, d the distance between the plates on which the drift voltage and radio-frequency field are applied, l_1 the distance from the electron beam to the end of the source region, and l_2 the length of the analyzer region. From the slopes of the linear plots and eq 23 and 24, the rate constants k_1 and k_2 are found to be

$$k_1 = 3.1 \times 10^{-10}\ \mathrm{cm^3\ molecule^{-1}\ sec^{-1}}$$

$$k_2 = 9 \times 10^{-12}\ \mathrm{cm^3\ molecule^{-1}\ sec^{-1}}$$

The rate constant k_1 for reaction 6 may be compared with the value 12×10^{-10} cm^3 molecule^{-1} sec^{-1} reported by Harrison, *et al.*,[24] for thermal ions by the pulse technique. An earlier determination gave 6.1×10^{-10} cm^3 molecule^{-1} sec^{-1}.[25,26] In a study of CH_4–D_2 and CD_4–H_2 systems, Lampe and Field[27] found the sum of

(24) S. K. Gupta, E. G. Jones, A. G. Harrison, and J. J. Myher, *Can. J. Chem.*, 45, 3107 (1967).
(25) A. G. Harrison, A. Ivko, and T. W. Shannon, *ibid.*, 44, 1351 (1966).
(26) A. G. Harrison, J. J. Myher, and J. C. J. Thynne, "Ion-Molecule Reactions in the Gas Phase," Advances in Chemistry Series, No. 58, P. J. Ausloos, Ed., American Chemical Society, Washington, D. C., 1966, p 150.
(27) F. W. Lampe and F. H. Field, *J. Am. Chem. Soc.*, 81, 3242 (1959).

the cross sections for reaction 7 and

$$D_2^+ + CH_4 \xrightarrow{k_3} CH_2D_2^+ + H_2 \quad (25)$$

to be much smaller than that for reaction 6; and Munson, *et al.*,[10] reported the sum of rate constants $k_2 + k_4$ of the reactions

$$CH_4^+ + D_2 \xrightarrow{k_2} CH_4D^+ + D \quad (26)$$

$$\xrightarrow{k_4} CH_2D_2^+ + H_2 \quad (27)$$

as 1.6–3.0 × 10^{-12} cm^3 molecule^{-1} sec^{-1}, and 0–7 × 10^{-12} cm^3 molecule^{-1} sec^{-1} for the rate k_5 of

$$CH_4^+ + H_2 \xrightarrow{k_5} CH_5^+ + H \quad (28)$$

at a field strength of 12.5 V/cm. Taking into account the difference in experimental conditions, we find that the values for k_1 and k_2 obtained in our work seem reasonable. Our value for k_1 is lower than others reported, but exactly the same value was obtained by us for reaction 6 in pure methane. With the same experimental conditions the rate constant for the reaction

$$D_2^+ + D_2 \longrightarrow D_3^+ + D \quad (29)$$

was found to be 5.2 × 10^{-10} cm^3 molecule^{-1} sec^{-1}, which is in good agreement with the value of 5.9 × 10^{-10} cm^3 molecule^{-1} sec^{-1} obtained by Harrison, *et al.*,[24-26] for thermal D_2^+ ions.

Discussion

1. Comparison of Observations with Previous Results from "High-Pressure" Mass Spectrometry. Despite the great differences in technique and experimental conditions, the same ionic deuterated reaction products are found in gaseous CH_4–D_2 systems by means of ion cyclotron resonance spectroscopy and "high-pressure" mass spectrometry. These species are CH_2D^+, CHD_2^+, CH_4D^+, CD_3^+, and the three partially deuterated ethyl ions, $C_2H_4D^+$, $C_2H_3D_2^+$, and $C_2H_2D_3^+$. However, the mechanisms involved in the isotopic exchange of deuterium for hydrogen atoms in carbon-containing ions could only be speculated in the previous work,[9,10] from variations of the intensities of the several ionic species with ionizing energy and with pressure and composition of the gaseous mixtures in the source chamber of the high-pressure mass spectrometer. The power of the method of ion cyclotron resonance spectroscopy, of course, is that it can delineate in an unambiguous manner the complex sequences of consecutive and competitive ion–molecule reactions taking place in these gaseous mixtures, but it is of considerable interest that the modes of reaction found in this study (Figure 5) confirm the mechanisms proposed earlier. In contrast to the lack of evidence in the earlier work for isotopic exchange in reactions of CH_5^+ with D_2, however, the present study definitely shows the following reaction to occur.

$$CH_5^+ + D_2 \longrightarrow CH_4D^+ + HD \quad (30)$$

The scavenging of CH_5^+ and CH_4D^+ by xenon probably occurs by a charge-transfer mechanism rather than by proton transfer, since the latter was not found in CH_4–Xe mixtures in Munson and Field's high-pressure mass spectrometer.[28] However, the strong quenching of D_3^+ should be due to both charge and proton transfer, as Aquilanti, *et al.*,[29] have observed XeH^+ in high yields in Xe–H_2 mixtures where H_2 was present in very high mole fraction. Our observation of efficient deuteron transfer from D_3^+ to methane confirms the results of Aquilanti and Volpi[11] for the H_2–CH_4 system at relatively high source pressures in their mass spectrometer.

It is of further interest to find that our results are evidence for the chain of ion–molecule reactions proposed by Firestone, Lemr, and Trudel[8] to account for the kinetics of formation between −21 and 123° of CH_3D in deuterium gas containing traces of CH_4. They suggested

$$D_2^+ + D_2 \longrightarrow D_3^+ + D \quad (31)$$

$$D_3^+ + CH_4 \longrightarrow CH_4D^+ + D_2 \quad (32)$$

$$CH_4^+ + D_2 \longrightarrow CH_4D^+ + D \quad (33)$$

$$CH_4D^+ + CH_4 \longrightarrow CH_5^+ + CH_3D \quad (34)$$

$$CH_5^+ + D_2 \longrightarrow CH_4D^+ + HD \quad (35)$$

$$CH_5^+ + e^- \longrightarrow CH_3 + H_2 \quad (36)$$

$$CH_4D^+ + e^- \longrightarrow CH_3 + HD \quad (37)$$

All the ion–molecule reactions 31 through 35 were observed in our work. However, we found no evidence for reactions of CH_4D^+ and CH_5^+ ions with methane to produce $C_2H_n^+$ products directly, reactions which they postulate. Collisional decomposition of protonated methane to methyl occurs, and the latter then combine with methane to give stable ethyl species.

2. The Mechanisms of Wilzbach Labeling of Methane. The labeling of gaseous methane with tritium, according to Pratt and Wolfgang,[6] takes place by three separate mechanisms. From kinetic and scavenger studies of mixtures of $CH_4 + T_2$ in the range of molecular ratios 10^3:1 to 10^4:1, they found the initial rate of formation of CH_3T, $R(CH_3T)$ in molecules cm^{-3} sec^{-1}, to be

$$R(CH_3T) = 9.2 \times 10^6[T_2] + 7.4 \times 10^7[T_2]^{3/2} + 7.8 \times 10^5[T_2]^2 \quad (38)$$

where $[T_2]$ is the concentration of tritium in millicuries per centimeter^3. The linear term in T_2 concentration was ascribed by them to production of CH_3T by a β decay-induced mechanism involving the reaction with methane of the $(THe^3)^+$ daughter from the nuclear transformation of T_2. The three-halves-power term in T_2 was attributed to a radiation-induced ionic species that has an electron recombination-limited lifetime. It was suggested that self-radiolysis of the gaseous mixture by β particles and secondary electrons ionized methane molecules, yielding mainly CH_4^+ and CH_3^+. The former primary species transferred a proton to CH_4 to give CH_5^+, and the latter was postulated to react with T_2

$$CH_5^+ + T_2 \longrightarrow CH_4T^+ + HT \quad (39)$$

in the rate-determining step responsible for the three-halves-power term in T_2 concentration in eq 38. The production of tritiated methane came about from

$$CH_4T^+ + CH_4 \longrightarrow CH_5^+ + CH_3T \quad (40)$$

Finally, the small term in the expression that varies with $[T_2]^2$ represents the effect of the radiation on the tritium component of the mixture. Since charge exchange of CH_5^+ with Xe is exoergic, the concentration of this ion should be very small when xenon is present. And in-

(28) M. S. B. Munson and F. H. Field, *J. Am. Chem. Soc.*, 87, 4242 (1965).

(29) V. Aquilanti, A. Galli, A. Giardini-Guidoni, and G. G. Volpi, *J. Chem. Phys.*, 43, 1969 (1965).

deed, addition of xenon to the mixture was observed to quench the $[T_2]^{3/2}$ term in the rate equation, but to leave unaffected the other two contributions to the rate of formation of CH_3T.

The ionic mechanism proposed by Pratt and Wolfgang to account for the fraction of labeled methane formed by reactions initiated by the $(THe^3)^+$ daughter of the β transformation of tritium is the following sequence.

$$T_2 \longrightarrow (THe^3)^+ + \beta^- \quad (41)$$

$$(THe^3)^+ + CH_4 \longrightarrow (CH_4T^+)^* + He^3 \quad (42)$$

$$(CH_4T^+)^* \longrightarrow CH_2T^+ + H_2 \quad (43)$$

$$CH_2T^+ + CH_4 \longrightarrow C_2H_4T^+ + H_2 \quad (44)$$

$$C_2H_4T^+ + e^- \longrightarrow \begin{cases} CH_2T + CH_2 \\ CHT + CH_3 \end{cases} \quad (45)$$

$$CH_2T + CH_4 \longrightarrow CH_3T + CH_3 \quad (46)$$

The $(CH_4T^+)^*$ ion was assumed to be excited and to dissociate quickly (in $\sim 10^{-11}$ sec), while the $C_2H_4T^+$ species was considered sufficiently long lived to be neutralized by electron capture. Tritiated methane was produced by H abstraction from methane by the CH_2T radical from the dissociative neutralization process. This mechanism was supported by the observations on $CH_4 + T_2 + D_2$ blends in a high-pressure mass spectrometer.[9] Direct evidence was obtained for the existence of the long-lived transient $C_2H_4T^+$ species, whereas CH_4T^+ was not found under conditions where the β's mostly escaped from the source chamber and thus only the primary effects of the nuclear decay could be observed. As Libby[30] has pointed out, since 1 mCi of T_2 corresponds to 3.7×10^7 dps, the value of the coefficient of the first term in eq 38 suggests that the efficiency of production of CH_3T by reactions beginning with the $(THe^3)^+$ daughter is about 25%. This molecular ion is found to be the reasonably long-lived decay product in 94.5% of the β transformations of T_2.[31] The presence of xenon would not be expected to interfere with the sequence of ionic reactions cited above, because those leading to $C_2H_4T^+$ are very fast, and charge exchange of the tritiated ethyl ion with Xe is endoergic. And, indeed, Pratt and Wolfgang found that the term linear in T_2 concentration was not quenched by Xe.

Our observations on CH_4–D_2 and CD_4–H_2 mixtures throw light on the ionic mechanisms involved in the predominant radiation-induced tritiation of methane; but to use the data it should be recognized at the outset that the ratio of methane to tritium in the conventional kinetics experiments of Pratt and Wolfgang was 10^3:1 to 10^4:1 and the total pressure was 675 Torr, whereas the concentrations of components in our experiments were comparable and the total pressure was much lower (10^{-3} to 10^{-5} Torr). Under the former conditions all CH_4^+ and CH_3^+ from the radiation of methane would have completely reacted to form CH_5^+ and $C_2H_5^+$, respectively, long before they would encounter T_2 molecules, since these reactions are very fast.[9,32]

The present studies by ion cyclotron resonance show that the $C_2H_5^+$ ion is completely inert toward D_2, and therefore would also be unreactive with T_2. Therefore, this long-lived species could not be involved in the formation of CH_3T by the modes denoted by the $[T_2]^{3/2}$ term. However, the CH_5^+ ion, which has been shown to be unreactive in methane,[33,34] can isotopically exchange hydrogen for deuterium when it encounters a D_2 molecule (Figure 5), and the CH_4D^+ product can reform CH_5^+ on meeting a CH_4. In addition, xenon strongly quenches both CH_5^+ and CH_4D^+ species (Figure 7). Consequently, both the double resonance spectra data and the results on Xe scavenging support the modes (eq 39 and 40) that account for the $[T_2]^{3/2}$ term in the over-all rate of formation of CH_3T.

Although Pratt and Wolfgang did not propose a mechanism of reactions initiated by ionization of the tritium component of their mixtures, the present work (Figure 5) indicates that the sequences of ionic reactions must be

$$T_2^+ + CH_4 \longrightarrow CH_4T^+ + T \quad (47)$$

$$CH_4T^+ \longrightarrow CH_2T^+ + H_2 \quad (48)$$

$$CH_2T^+ + CH_4 \longrightarrow C_2H_4T^+ + H_2 \quad (49)$$

followed by reactions 45 and 46. Although CH_4T^+ is strongly quenched by xenon when the concentrations of gases are comparable (Figure 7), the scavenging action would probably not be observable in Pratt and Wolfgang's systems, in which the over-all pressure was 675 Torr and Xe was present in ~5% abundance. The sequences of consecutive ion–molecule reactions (47–49) would be completed before they could be interfered with by xenon atoms.

The behaviors of the various ionic species in the presence of nitric oxide were quite similar to their respective behaviors with xenon. Consequently, the only explanation of Pratt and Wolfgang's observation of complete quenching of all three mechanisms by NO must be its scavenging of tritiated methyl radicals formed in reaction 45 in addition to ionic scavenging of CH_4T^+ and CH_5^+.

In conclusion, our studies using ion cyclotron resonance spectroscopy, in combination with the previous results from high-pressure mass spectrometry, offer fairly convincing evidence for the mechanisms proposed by Pratt and Wolfgang as being responsible for the self-induced tritiation of methane.

(30) W. F. Libby, "The Mechanism of the Self-Induced Labelling of Methane by Tritium Gas," unpublished.
(31) S. Wexler, *J. Inorg. Nucl. Chem.*, 10, 8 (1959); see also A. H. Snell F. Pleasonton, and H. E. Leming, *ibid.*, 5, 112 (1957).
(32) S. Wexler and N. Jesse, *J. Am. Chem. Soc.*, 84, 3425 (1962).
(33) F. H. Field and M. S. B. Munson, *ibid.*, 87, 3289 (1965).
(34) S. Wexler, A. Lifshitz, and A. Quattrochi in ref 26, p 193.